

# Anisotropic RKKY interaction in spin polarized graphene

F. Parhizgar,<sup>1</sup> Reza Asgari,<sup>1,\*</sup> Saeed H. Abedinpour,<sup>2</sup> and M. Zareyan<sup>2</sup>

<sup>1</sup>*School of Physics, Institute for Research in Fundamental Sciences (IPM), Tehran 19395-5531, Iran*

<sup>2</sup>*Department of Physics, Institute for Advanced Studies in Basic Sciences (IASBS), Zanjan 45137-66731, Iran*

(Dated: October 18, 2018)

We study the Ruderman-Kittle-Kasuya-Yosida (RKKY) interaction in the presence of spin polarized two dimensional Dirac fermions. We show that a spin polarization along the  $z$ -axis mediates an anisotropic interaction which corresponds to a XXZ model interaction between two magnetic moments. For undoped graphene, while the  $x$  part of interaction keeps its constant ferromagnetic sign, its  $z$  part oscillates with the distance of magnetic impurities,  $R$ . A finite doping causes that both parts of the interaction oscillate with  $R$ . We explore a beating pattern of oscillations of the RKKY interaction along armchair and zigzag lattice directions, which occurs for some certain values of the chemical potential. The two characteristic periods of the beating are determined by inverse of the difference and the sum of the chemical potential and the spin polarization.

PACS numbers: 75.30.Hx, 75.10.Lp, 75.10.Jm, 75.30.Ds

## I. INTRODUCTION

The charge and spin oscillatory interactions in metals has attracted considerable attention both on the theoretical and experimental sides<sup>1,2</sup>. Ruderman and Kittle<sup>3</sup> suggested that the spin oscillatory interaction in metals could provide a long-range interaction between nuclear spins in metals. Afterwards, Kasuya and Yosida<sup>4</sup> extended the theory to include the long-range interaction between magnetic impurities and thus the combined refers to RKKY interaction.

The recent discovery of graphene<sup>5</sup>, the two-dimensional crystal of carbon atoms, has provided a new material with a peculiar structure for the charge and the spin interactions. This stable crystal has already attracted considerable attention because of its unusual effective many-body properties<sup>6-13</sup> that follow from chiral nature of linearly dispersing low energy excitations described by pair of Dirac cones at the  $K$  and  $K'$  edges of the first Brillouin zone.

The RKKY interaction in pristine graphene has been studied by several groups<sup>14-16</sup>. Due to the particle-hole symmetry of graphene, the RKKY interaction induces ferromagnetic correlation between magnetic impurities on the same sublattice, while anti-ferromagnetic correlation between the ones on different sublattices. The dependence of the interaction on the distance  $R$  between two local magnetic moments, at the Dirac point, is found to be  $R^{-3}$ , whereas it behaves as  $R^{-2}$  in conventional two-dimensional (2D) systems<sup>17</sup>. Such a fast decay rate denotes that the interaction is rather short-ranged. In doped graphene, on the other hand, the spacial depen-

dence of the interaction is predicted to be similar to conventional 2D systems, but this still remains to be experimentally verified.

Due to the fact that the RKKY interaction is originated by the exchange coupling between the impurity moments and the spin of itinerant electrons in the bulk of the system, spin polarization of electrons is expected to influence directly this interaction<sup>18</sup>. In particular, combination of the spin-dependence with a Dirac-like spectrum can mediate a much richer collective behavior of magnetic adatoms<sup>19</sup>. This has been explained for surface states of a three dimensional topological insulator, on which magnetic impurities exhibit a frustrated RKKY interaction with two possible phases of ordered ferromagnetic phase and a disordered spin glass phase<sup>20</sup>. Graphene, in particular, with imbalanced chemical potentials of spin-up and spin-down electrons, presents a unique spin chiral material in which the interplay between the spin polarization, gapless spectrum, and the chiral nature of electrons have been shown to result intriguing phenomena<sup>21</sup>. In two-dimension graphene system, the polarization of the chemical potential can be tuned to be of order or even higher than the mean chemical potential, the condition which is not possible in ordinary conductors. The aim of the present study is to address the question of how this peculiarity can affect the collective coupling of magnetic impurities on the surface of graphene sheet with a finite polarization of the spin.

In this work, we calculate the RKKY interaction mediated by spin-polarized Dirac fermions in a monolayer graphene using the Green's function method. Our theory for the spin polarization dependence of RKKY interac-

tion is motivated not only by fundamental transport considerations, but also by application and potential future experiments in graphene spintronic field. With a spin-polarization along the  $z$ -axis, we show that the RKKY interaction is anisotropic corresponding to a XXZ model interaction between the two magnetic moments when their spin orientations are fixed. Besides  $R^{-3}$  dependence of the interaction for undoped graphene, we show particularly that the interaction behaves like  $R^{-2}$  when the spin polarization is finite. In addition, a beating pattern for the interaction in the cases where impurities are located along certain directions is obtained near the resonance condition which is controlled by the chemical potential and the spin polarization.

The paper is organized as the following. In Sec. II we introduce the formalism that will be used in calculating the RKKY interaction from the lattice Green's function. In Sec. III we present our analytic and numeric results for the coupling strengths of the RKKY interaction in both undoped and doped graphene sheets. Sec. IV contains discussions and a brief summary of our main results.

## II. METHOD AND THEORY

We consider a spin-polarized graphene system identified by a spin dependent chemical potential  $\mu_s$  ( $s = \pm 1$ ), implying a mean chemical potential  $\mu = \sum_s \mu_s/2$  and the spin polarization  $\mu_p = \sum_s s\mu_s/2$ . Such a spin-polarization can be injected, for instance, by ferromagnetic electrodes on top of the graphene sheet<sup>22,23</sup>. Intrinsic ferromagnetic correlations are also predicted to exist in graphene sheets<sup>24</sup> and nanoribbons with zigzag edges<sup>25</sup> under certain conditions.

The electronic structure of spin polarized graphene can be reasonably well described using a rather simple tight-binding Hamiltonian, leading to analytical solutions for their energy dispersion and related eigenstates. The non-interacting nearest neighbor tight-binding Hamiltonian for  $\pi$ -band electrons with spin  $s$ , is determined by<sup>26</sup>

$$\hat{\mathcal{H}}_0^s = -t \sum_{\langle i,j \rangle} \left( a_{i,s}^\dagger b_{j,s} + b_{i,s}^\dagger a_{j,s} \right) - s\mu_p \sum_i \left( a_{i,s}^\dagger a_{i,s} + b_{i,s}^\dagger b_{i,s} \right), \quad (1)$$

where  $a_{i,s}$  ( $b_{i,s}$ ) annihilates an electron with spin  $s$  on sublattice A(B) of unit cell  $i$  and  $t \simeq 2.9$  eV denotes the nearest neighbor hopping parameter<sup>27</sup>. The sum  $\langle i,j \rangle$  in

Eq. (1) runs over distinct nearest neighbors.

The  $s$ -component of the noninteracting Hamiltonian in momentum space is written as

$$\hat{\mathcal{H}}_0^s = \begin{pmatrix} -s\mu_p & f(\mathbf{k}) \\ f^*(\mathbf{k}) & -s\mu_p \end{pmatrix}, \quad (2)$$

where the form factor in general case is  $f(\mathbf{k}) = -t \sum_j e^{i\mathbf{k} \cdot \mathbf{d}_j}$ , in which  $\mathbf{d}_j$ 's are nearest neighbor position vectors. In this work, we are interested in the low-energy behavior, in which  $f(\mathbf{k}) = v_F k \Phi(k)$ , where  $\Phi(k) = e^{i(\pi/3+\theta_k)}$  at the Dirac point  $K$  and  $\Phi(k) = -e^{i(\pi/3-\theta_k)}$  at the another Dirac point,  $K'$ , the chiral angle is  $\theta_k = \tan^{-1}(k_x/k_y)$ ,  $v_F = 3ta/2\hbar \simeq 10^6$  m/s is the Fermi velocity with  $a \simeq 1.42\text{\AA}$  being the Carbon-Carbon distance in honeycomb lattice.

Our system incorporates two localized magnetic moments whose interaction is mediated through a spin polarized electron liquid. We assume that the graphene is spin polarized first, and then we add the magnetic moments. The contact interaction between the spin of itinerant electrons and two magnetic impurities with magnetic moments  $\mathbf{M}_1$  and  $\mathbf{M}_2$ , located respectively at  $\mathbf{R}_1$  and  $\mathbf{R}_2$ , is given by

$$\hat{\mathcal{H}}_{\text{int}} = \lambda \sum_{j=1,2} \mathbf{M}_j \cdot \mathbf{s}(\mathbf{R}_j), \quad (3)$$

where  $\lambda$  is the coupling constant between conduction electrons and impurity,  $\mathbf{s}(\mathbf{r}) = \frac{\hbar}{4} \sum_i \delta(\mathbf{r}_i - \mathbf{r}) \boldsymbol{\sigma}_i$  is the spin density operator<sup>1</sup> with  $\mathbf{r}_i$  and  $\boldsymbol{\sigma}_i$  being the position and vector of spin operators of  $i$ th electron.

The RKKY interaction which arises from the quantum effects is obtained by using a second order perturbation<sup>3,4,29</sup> which reads as (from now on we set  $\hbar = 1$ )

$$\hat{\mathcal{H}}_{\text{RKKY}}^{\alpha\beta} = \frac{-\lambda^2}{\pi} \Im m \int_{-\infty}^{\infty} d\varepsilon \text{Tr}[(\mathbf{M}_1 \cdot \boldsymbol{\sigma}) G_{\alpha\beta}(\mathbf{R}_1, \mathbf{R}_2; \varepsilon) \times (\mathbf{M}_2 \cdot \boldsymbol{\sigma}) G_{\beta\alpha}(\mathbf{R}_2, \mathbf{R}_1; \varepsilon)] n(\mu), \quad (4)$$

where  $n(\mu)$  denotes the Fermi-Dirac distribution function,  $\boldsymbol{\sigma}$  is the vector of Pauli matrices in the *spin* space,  $G_{\alpha\beta}(\mathbf{R}_1, \mathbf{R}_2; \varepsilon)$  is a  $2 \times 2$  matrix of the single particle retarded Green's function in spin space, and  $\alpha$  and  $\beta$  refer to the sublattices where two impurities are placed and finally, the trace is taken over the spin degree of freedom.

For spin unpolarized graphene, Eq. (4) simplifies to  $\hat{\mathcal{H}}_{\text{RKKY}}^{\alpha\beta} = \frac{\lambda^2}{4} \chi(\mathbf{R}_1, \mathbf{R}_2) \mathbf{M}_1 \cdot \mathbf{M}_2$ , where  $\chi(\mathbf{R}_1, \mathbf{R}_2)$  is the spin susceptibility of the itinerant electrons and determines the indirect interaction between two local moments.

In order to calculate the interaction Hamiltonian of Eq. (4), the form of the electronic single particle Green's function,  $G^s(\mathbf{R}_1, \mathbf{R}_2; \varepsilon) = \langle \mathbf{R}_1 | (\varepsilon + i0^+ - \hat{\mathcal{H}}_0^s)^{-1} | \mathbf{R}_2 \rangle$  is needed. To calculate the retarded Green's function in real space, its Fourier components in momentum space might be first obtained. Due to the fact that our 2D Dirac fermion system is noninteracting and thus the direction of spin remains unchanged, the retarded Green's function  $G_{\alpha\beta}$  are diagonal in the spin space

$$G_{AA}^s(\mathbf{R}, 0, \varepsilon) = (e^{i\mathbf{K}\cdot\mathbf{R}} + e^{i\mathbf{K}'\cdot\mathbf{R}})g_{AA}(\varepsilon - s\mu_p), \quad (5)$$

and

$$G_{AB}^s(\mathbf{R}, 0, \varepsilon) = e^{i\pi/3}(e^{i\mathbf{K}\cdot\mathbf{R}+i\theta_R} - e^{i\mathbf{K}'\cdot\mathbf{R}-i\theta_R}) \times g_{AB}(\varepsilon - s\mu_p). \quad (6)$$

Moreover,  $G_{BB}^s = G_{AA}^s$  and  $G_{BA}^s(0, \mathbf{R}, \varepsilon) = \exp(-i\pi/3)(\exp(-i\mathbf{K}\cdot\mathbf{R} - i\theta_R) - \exp(-i\mathbf{K}'\cdot\mathbf{R} + i\theta_R))g_{AB}(\varepsilon - s\mu_p)$ . Here  $g_{AA}(\varepsilon) = \gamma\varepsilon K_0(-i\varepsilon R/v_F)$  and  $g_{AB}(\varepsilon) = \gamma\varepsilon K_1(-i\varepsilon R/v_F)$ , where  $K_0(x)$  and  $K_1(x)$  are the modified Bessel functions of the second kind,  $\theta_R$  is the angle of the position  $\mathbf{R}$  with respect to the  $\mathbf{K}' - \mathbf{K}$  direction and  $\gamma = -2\pi/(\Omega v_F^2)$ , in which  $\Omega$  is the area of the Brillouin zone.

By inserting the retarded Green's functions given by Eqs. (5) and (6) in Eq. (4), and taking the trace over spin degree of matrices, the RKKY Hamiltonian simplifies to

$$\mathcal{H}_{\text{RKKY}}^{\alpha\beta} = \frac{\lambda^2}{\pi} [J_x^{\alpha\beta}(M_{1x}M_{2x} + M_{1y}M_{2y}) + J_z^{\alpha\beta}M_{1z}M_{2z}], \quad (7)$$

which is the honored XXZ model. Here  $J_x^{\alpha\beta} = -C\Phi_{\alpha\beta}I_x^{\alpha\beta}/R^3$  and  $J_z^{\alpha\beta} = -C\Phi_{\alpha\beta}I_z^{\alpha\beta}/R^3$ , with  $C = 2(2\pi)^2/\Omega^2 v_F$ ,  $\Phi_{AA} = 1 + \cos[(\mathbf{K} - \mathbf{K}')\cdot\mathbf{R}]$  and  $\Phi_{AB} = -1 + \cos[(\mathbf{K} - \mathbf{K}')\cdot\mathbf{R} + 2\theta_R]$ . The different components of  $I^{\alpha\beta}$  for impurities on the same sublattice read as

$$I_x^{AA} = 2\Im \left[ \int_{-\infty}^{y_F} dy x_- K_0(-ix_-) x_+ K_0(-ix_+) \right], \quad (8)$$

$$I_z^{AA} = \Im \left[ \int_{-\infty}^{y_F} dy \sum_{s=\pm} x_s^2 K_0^2(-ix_s) \right],$$

where  $y_F = \mu R/v_F$ ,  $x_{\pm} = y \pm h_F$ ,  $y = \varepsilon R/v_F$ , and  $h_F = \mu_p R/v_F$ . For impurities on different sublattices, one only needs to replace  $K_0(x)$  with  $K_1(x)$  in the above equations. Note that  $J^{BB} = J^{AA}$  and  $J^{BA} = J^{AB}$ .

We find analytic results for the  $z$  component of the RKKY exchange coupling strength  $I_z$ , for both cases

where magnetic moments are located on the same or different sublattices. For the same sublattice case, we begin by splitting the integral in the second line of Eq. (8) into the conduction and valance band contributions, and find

$$I_z^{AA}(R) = 2\Im \left[ \int_{-\infty}^0 dx x^2 K_0^2(-ix) \right] + \sum_{s=\pm} \Im \left[ \int_0^{x_{Fs}} dx x^2 K_0^2(-ix) \right], \quad (9)$$

where  $x_{F\pm} = y_F \pm h_F$ . The first integral can be solved<sup>15,16</sup> easily and the result is  $\pi^2/32$ . The contribution from the second line of Eq. (9), can be also obtained by replacing  $\Im[K_0^2(-ix)]$  with  $-\pi^2 \text{sign}(x) J_0(|x|) Y_0(|x|)/2$ , and using the following relation

$$\int_0^{x_F} dx x^2 \text{sign}(x) J_0(|x|) Y_0(|x|) = -\frac{|x_F|}{2\sqrt{\pi}} M(x_F), \quad (10)$$

where  $M(x) = G[\{\{\frac{1}{2}\}, \{\frac{3}{2}\}\}, \{\{1, 1\}, \{-\frac{1}{2}, 1\}\}, x^2]$  is Meijer  $G$ -function<sup>30</sup>. As a result, the function  $I_z^{AA}$  is given by

$$I_z^{AA}(R) = \frac{\pi^2}{4} \sum_{s=\pm} \left[ \frac{1}{8} + \frac{|x_{Fs}|}{\sqrt{\pi}} M(x_{Fs}) \right]. \quad (11)$$

To calculate the long-range behavior of the RKKY interaction, the asymptotic behavior of the Meijer  $G$ -function is needed. It is also easy to see that asymptotic behavior of  $M(x)$  at large  $x$  is<sup>30</sup>  $[2\cos(2x) + 8x\sin(2x) - \pi]/(8\sqrt{\pi}x)$ . It should be noticed that the  $M(x)$  tends to its long-range asymptotic expression for  $x > 2$ . Therefore,  $I_z^{AA}(R)$  for the long-range regime is simplified as

$$I_z^{AA}(R \gg a) \approx \frac{\pi}{16} \sum_{s=\pm} [\cos(2x_{Fs}) + 4x_{Fs}\sin(2x_{Fs})] \quad (12)$$

On the other hand, for the case that the impurities are located on two different sublattices we can follow the same procedure discussed above, while we use  $\int_{-\infty}^0 dx x^2 \Im[K_1^2(-ix)] = 3\pi^2/32$ , and  $\Im[K_1^2(-ix)] = \pi^2 \text{sign}(x) J_1(|x|) Y_1(|x|)/2$  to find

$$\int_0^{x_F} dx x^2 \text{sign}(x) J_1(|x|) Y_1(|x|) = -\frac{|x_F|}{2\sqrt{\pi}} M'(x_F), \quad (13)$$

where  $M'(x) = G[\{\{\frac{1}{2}\}, \{\frac{3}{2}\}\}, \{\{1, 2\}, \{-\frac{1}{2}, 0\}\}, x^2]$ . Finally the  $I_z^{AB}(R)$  reads as

$$I_z^{AB}(R) = \frac{\pi^2}{4} \sum_{s=\pm} \left[ \frac{3}{8} - \frac{|x_{Fs}|}{\sqrt{\pi}} M'(x_{Fs}) \right]. \quad (14)$$

The asymptotic behavior of  $M'(x)$  at large  $x$  is  $[3\pi -$

$10 \cos(2x) - 8x \sin(2x)] / (8\sqrt{\pi}|x|)$ . Therefore, the long-range behavior of  $I_z^{AB}$  is obtained as

$$I_z^{AB}(R \gg a) \approx \frac{\pi}{16} \sum_{s=\pm} [5 \cos(2x_{Fs}) + 4x_{Fs} \sin(2x_{Fs})] . \quad (15)$$

It should be mentioned that we were not able to find simple analytic expressions for the in plane components of the exchange coupling,  $I_x^{\alpha\beta}$  and in the next section we will present our numerical results of them.

### III. NUMERICAL RESULTS AND DISCUSSIONS

In this section, we present our main results for the RKKY exchange coupling in the presence of a spin polarization Dirac fermions along the  $z$ -axis by analyzing the above calculated integrals of  $I_x$  and  $I_z$ . We extend the previously studied<sup>16</sup> results for dependencies on the distance  $R$  and lattice direction  $\theta_R$  to the case of  $\mu_p \neq 0$ , for two different regimes of undoped, ( $\mu = 0$ ) and doped, ( $\mu \neq 0$ ) graphene.

For the  $I_z$  component of interactions, we solve the two expressions in Eqs. (11) and (14), numerically and then compare the results with asymptotic results obtained from the analytical expressions given by Eqs. (12) and (15), respectively. Generally, the results obtained from the two approaches match quite good in most of the case specially at long distances. The distance dependence of  $I_z$  for both AA and AB cases are illustrated in Fig. 1 for the undoped graphene. For an unpolarized graphene  $\mu_p = 0$ ,  $I_z^{AA} = I_x^{AA}$  is just a constant. At finite  $\mu_p$ , the integral  $I_z$  has quite different behavior exhibiting an oscillatory behavior as a function of  $R$ , with a linearly growing amplitude and a period given by  $2\pi/h_F$ , as can be obtain directly from Eq. (12). This behavior of  $I_z^{AA}$  results in an oscillatory  $J_z^{AA}$  with a decreasing amplitude as  $R^{-2}$ , which mimics the behavior of the RKKY coupling of an unpolarized doped graphene<sup>16</sup>. We can understand this analogy by noting that the polarization induces spin-dependent doping of up and down spin Dirac bands of an undoped sample by shifting their chemical potential from the Dirac point. A comparison between  $R$ -dependence of the integral  $I_z^{AA}$  and that of  $I_z^{AB}$  for various values of  $\mu_p$  in Fig. 1(b), shows their difference at short distance while reaching each other as  $R$  increases. As  $R \rightarrow 0$  the coupling interactions tend to their values of the unpolarized case where  $J^{AB}$  is three times larger

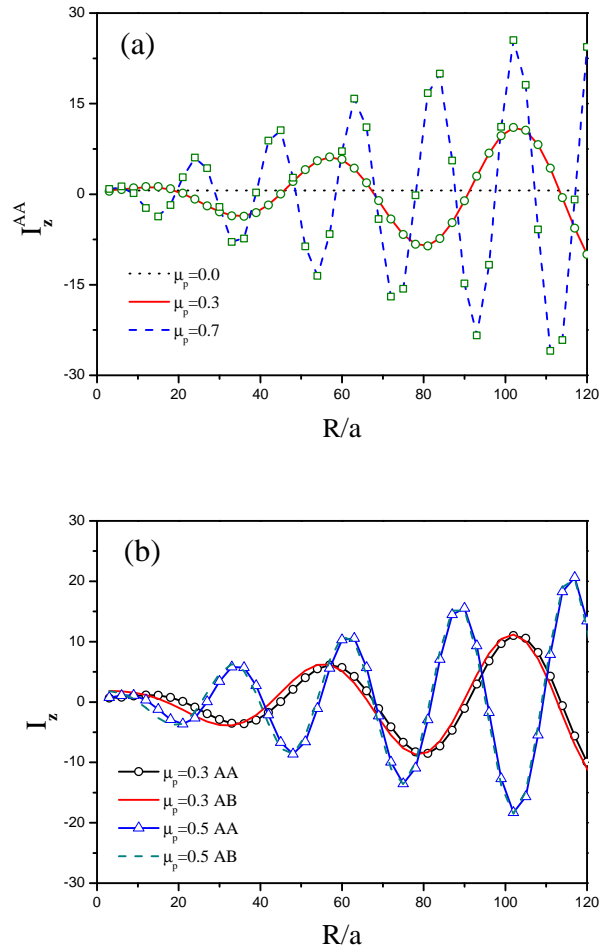


FIG. 1: (Color online) (a) The integral  $I_z^{AA}$  as a function of the distance  $R$  when both impurities are located on the same sublattice for various values of the spin polarization,  $\mu_p$  in units of eV. The chemical potential is set to zero. Symbols refer to the analytical results of Eq. (12) which are compared to the numerical evaluation of Eq. (11), plotted as lines. For  $\mu_p = 0$ ,  $I_z^{AA} = I_z^{AB}$  is just a constant. (b) A comparison between the integral  $I_z^{AA}$  and  $I_z^{AB}$  as a function of the distance  $R$  for various values of the spin polarization  $\mu_p$  in units of eV. At finite  $\mu_p$ , the integral  $I_z$  has a quite different behavior, oscillating as a function of  $R$ , with a period given by  $2\pi/h_F$  and a linearly growing amplitude. A comparison between  $R$ -dependence of the integral  $I_z^{AA}$  and that of  $I_z^{AB}$ , shows their difference at short distance while reaching each other as  $R$  increases.

than  $J^{AB}$ , as is discussed in Ref. [16].

From the numerical calculations of the integrals appearing in Eq. (8), we can also obtain the behavior of  $I_x^{AA}$  and  $I_x^{AB}$  for the RKKY interaction coupling of the components of the magnetic moments which are perpendicular to the spin polarization axis. Fig. 2(a) shows  $I_x^{AA}$  as a function of  $R$  for the undoped graphene at different

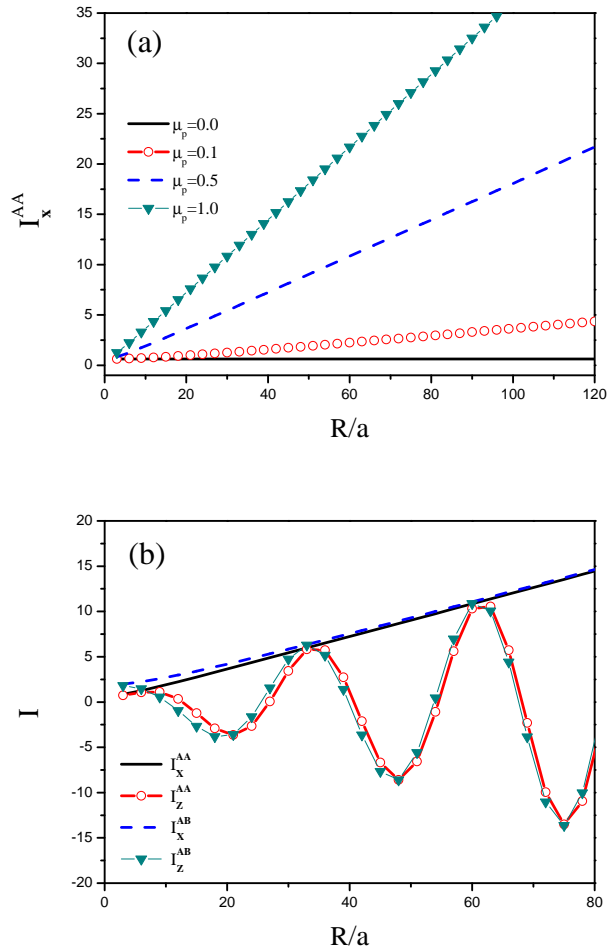


FIG. 2: (Color online) (a) The integral  $I_x^{AA}$  versus distance between two impurities, when both impurities are located on the same sublattice for undoped graphene and for several values of  $\mu_p$  in units of eV. Finite  $\mu_p$ , produces a linear increase of  $I_x^{AA}$  with a slope proportional to  $\mu_p$ . (b) A comparison between  $I_x$  and  $I_z$  for different configurations and for  $\mu_p = 0.5$  eV.

values of the spin polarization,  $\mu_p$ . For  $\mu_p = 0$ , this function is a constant resulting a  $J_x^{AA}$  which decays as  $R^{-3}$ . A finite difference  $\mu_p$  between the chemical potentials of spin up and spin down carriers, produces a linear increase of  $I_x^{AA}$  with a slope proportional to  $\mu_p$ . Thus,  $J_x^{AA}$  decays as  $R^{-2}$ . Importantly, the sign of interaction  $J_x^{AA}$  is always positive which shows that the coupling between the perpendicular components of the moments remains ferromagnetic-like for all  $R$ s. To analyze the difference between the two configurations of AA and AB, in Fig. 2(b) we have compared  $I_x^{AA}$  and  $I_x^{AB}$ , which shows that despite the difference at short distances, they tend to each other at larger distances.

At finite values of both the chemical potential and the spin polarization, more complicated behavior of the RKKY coupling can be occurred. In this case, the behavior of  $I_z$  is determined by a superposition of four sinusoidal functions with two different periods of  $2\pi R/(x_{F-})$  and  $2\pi R/(x_{F+})$  each occurring twice with amplitudes  $1, x_{F-}$  and  $1, x_{F+}$ , respectively. As the result, we observe that for certain values of  $\mu$  and  $\mu_p$ , oscillations of  $I_z$  exhibit a beating pattern with two characteristic periods. Fig. 3(a) shows this beating behavior of integral,  $I_z^{AA}$  as a function of the impurities distance along armchair direction (where  $R = 3na$  with  $n$  being an integer number) for  $\mu = 1.2$  eV and  $\mu_p = 1.0$  eV. Fig. 3(b) shows the similar behavior of integral  $I_z^{AA}$  as a distance along zigzag direction (where  $R = \sqrt{3}ma$  for an integer  $m$ ) for  $\mu = 1.2\sqrt{3}$  eV and  $\mu_p = \sqrt{3}$  eV. We have obtained a similar beating pattern for oscillations of  $I_z^{AB}$ , which also occurs for a certain values of  $\mu$  and  $\mu_p$ .

The behavior of the perpendicular components  $I_x$  for  $\mu \neq 0$  is also different from their linear behavior of the undoped case, as it is shown in Fig. 4(a) for the fixed value of  $\mu = 0.5$  eV and different values of  $\mu_p$ . In this case  $I_x(R)$  exhibits oscillations with a linearly increasing amplitude whose slope is proportional to  $|\mu - \mu_p|$ . Fig. 4(b) is the same as Fig. 4(a), but this time  $\mu_p$  is fixed and  $\mu$  changes.

#### IV. SUMMARY AND CONCLUSIONS

In conclusion, we have studied the influence of spin polarization on RKKY interaction in graphene. With a spin polarization along the  $z$ -axis, the induced interaction between two magnetic impurities is found to be described by an anisotropic XXZ Hamiltonian with an exchange coupling depending on the distance  $R$  between the impurities and the doping level. For undoped but spin-polarized graphene, we have found that while the interaction between the  $x$  components of the moments remains constant with ferromagnetic sign, for the  $z$  components it oscillates with the distance  $R$ . In unpolarized spin case, the RKKY interaction induces ferromagnetic correlation between magnetic impurities on the same sublattice, while anti-ferromagnetic correlation between the ones on different sublattices<sup>14-16</sup>. The dependence of the interaction on the distance  $R$  between two local magnetic moments, at the Dirac point, is found to be  $R^{-3}$ , whereas it behaves as  $R^{-2}$  in doped graphene sheet. Besides  $R^{-3}$

Chemical potential	Spin polarization	Coupling of strength interaction
$\mu = 0$	$\mu_p = 0$	$J^{AA} \propto -R^{-3}$ $J^{AB} \propto R^{-3}$
$\mu \neq 0$	$\mu_p = 0$	$J^{AA} \propto -\sin(2k_F R + \alpha)R^{-2}$ $J^{AB} \propto \sin(2k_F R + \beta)R^{-2}$
$\mu = 0$	$\mu_p \neq 0$	$J_x^{AA} \propto -\mu_p R^{-2}$ $J_z^{AA} \propto -\sin(2k_h R)\mu_p R^{-2}$ $J_x^{AB} \propto \mu_p R^{-2}$ $J_z^{AB} \propto +\sin(2k_h R)R^{-2}$
$\mu \neq 0$	$\mu_p \neq 0$	$J_x^{AA} \propto -\sin(2k_F R)R^{-2}$ $J_z^{AA} \propto -(\sin(2x_{F+}) + C \sin(2x_{F-}))R^{-2}$ $J_x^{AB} \propto \sin(2k_F R)R^{-2}$ $J_z^{AB} \propto (\sin(2x_{F+}) + C \sin(2x_{F-}))R^{-2}$

TABLE I: A breakdown of the results on the scaling form of the RKKY interactions in monolayer graphitic systems. The results for vanishing spin polarization are reported from Ref. [16] while the ones for finite spin polarization denote to present work. It is worthwhile mentioning that the interaction Hamiltonian is modelled by the Heisenberg model for  $\mu_p = 0$  and by the  $XXZ$  model for the case that  $\mu_p \neq 0$ . We introduce a parameter  $k_h = \mu_p/v_F$  and  $C = (\mu - \mu_p)/(\mu + \mu_p)$  which are given by the chemical potential as well as the spin polarization.

dependence of the interaction for undoped graphene, we show particularly that the interaction behaves like  $R^{-2}$  when the spin polarization is finite.

At finite value of both the chemical potential and the spin polarization, more complicated behavior of the RKKY coupling can be occurred. We have found that both components of the interaction oscillate with  $R$ . We have explored that for the chemical potentials  $\mu$  close to the polarization  $\mu_p$ , oscillations of the RKKY interaction exhibit a beating pattern when the impurities are located along zigzag or armchair directions. The two characteristic periods of the beating oscillations are determined by

inverse of the difference and the sum of the chemical potential and the spin polarization. Since several works on RKKY interaction in 2D graphene systems are available, a proper comparison with those results seems to be in order (see Table I).

## V. ACKNOWLEDGMENTS

We are grateful to Jahanfar Abouie for useful discussions. This work is partially supported by IPM grant.

\* Electronic address: asgari@ipm.ir

<sup>1</sup> G. F. Giuliani and G. Vignale, *Quantum Theory of the Electron Liquid* (Cambridge University Press, Cambridge, 2005).

<sup>2</sup> M. W. Wu, J. H. Jiang, and M. Q. Weng, *Phys. Rep.* **493**, 61 (2010).

<sup>3</sup> M. A. Ruderman and C. Kittel, *Phys. Rev.* **96**, 99 (1954).

<sup>4</sup> T. Kasuya, *Prog. Theor. Phys.* **16**, 45 (1956); K. Yosida, *Phys. Rev.* **106**, 893 (1957).

<sup>5</sup> K. S. Novoselov, A. K. Geim, S. V. Morozov, D. Jiang, Y. Zhang, S. V. Dubonos, I. V. Grigorieva, and A. A. Firsov, *Science* **306**, 666 (2004).

<sup>6</sup> A. Bostwick, F. Speck, T. Seyller, K. Horn, M. Polini, R. Asgari, A. H. MacDonald, and E. Rotenberg, *Science* **328**, 999 (2010).

<sup>7</sup> Y. Barlas, T. Pereg-Barnea, M. Polini, R. Asgari, and A. H. MacDonald, *Phys. Rev. Lett.* **98**, 236601 (2007).

<sup>8</sup> M. Polini, R. Asgari, Y. Barlas, T. Pereg-Barnea, and A. H. MacDonald, *Solid State Commun.* **143**, 58 (2007).

<sup>9</sup> M. Polini, R. Asgari, G. Borghi, Y. Barlas, T. Pereg-

Barnea, and A. H. MacDonald, *Phys. Rev. B* **77**, 081411(R) (2008); E. H. Hwang and S. Das Sarma, *ibid* **77**, 081412 (2008); A. Qaiumzadeh and R. Asgari, *New J. Phys.* **11**, 095023 (2009).

<sup>10</sup> F. de Juan, A. G. Grushin, and M. A. H. Vozmediano, *Phys. Rev. B* **82**, 125409 (2010); P. E. Trevisanutto, C. Giorgetti, L. Reining, M. Ladisa, and V. Olevano, *Phys. Rev. Lett.* **101**, 226405 (2008); R. Roldán, M. P. López-Sancho, and F. Guinea, *Phys. Rev. B* **77**, 115410 (2008).

<sup>11</sup> R. Asgari, M. M. Vazifeh, M. R. Ramezani, E. Davoudi, and B. Tanatar, *Phys. Rev. B* **77**, 125432 (2008).

<sup>12</sup> V. N. Kotov, B. Uchoa, V. M. Pereira, A. H. Castro Neto, and F. Guinea, *Rev. Mod. Phys.* **84**, 1067 (2012).

<sup>13</sup> A. Qaiumzadeh, Kh. Jahanbani, and R. Asgari, *Phys. Rev. B* **85**, 235428 (2012).

<sup>14</sup> M. A. H. Vozmediano, M. P. López-Sancho, T. Stauber, and F. Guinea, *Phys. Rev. B* **72**, 155121 (2005); D. A. Abanin, A. V. Shytov, and L. S. Levitov, *Phys. Rev. Lett.* **105**, 086802 (2010); A. M. Black-Schaffer, *Phys. Rev. B* **82**, 073409 (2010); *ibid* **84**, 125416 (2011); S. R. Power,

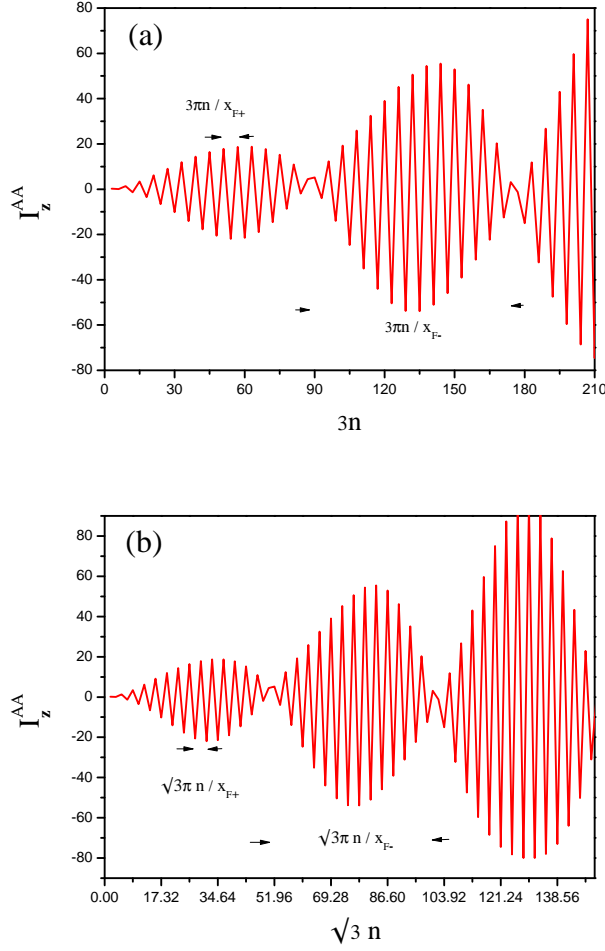


FIG. 3: (Color online) (a) The integral  $I_z^{AA}$  as a function of the impurities distance along armchair direction when both impurities are located on the same sublattice. The existence of two different periods in doped polarized graphene for certain values of  $\mu = 1.2$  eV and  $\mu_p = 1.0$  eV is clear in this figure. (b) The integral  $I_z^{AA}$  as a distance along zigzag direction for  $\mu = 1.2\sqrt{3}$  eV and  $\mu_p = \sqrt{3}$  eV.

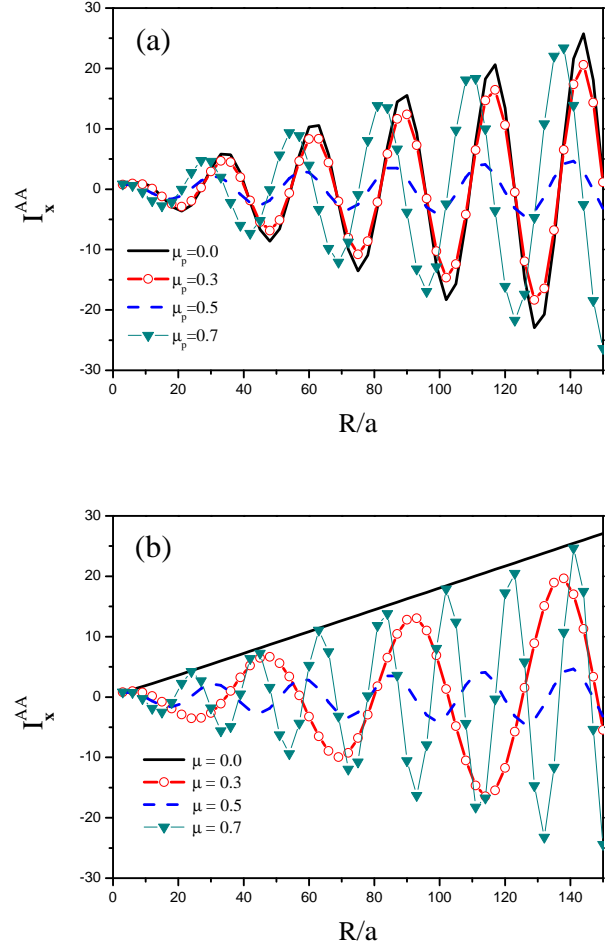


FIG. 4: (Color online) (a) The integral  $I_x$  versus distance between two impurities, when both impurities are on the same sublattice for doped graphene with the chemical potential 0.5 eV and various value of  $\mu_p$  in units of eV. (b) Same as (a) but for fixed  $\mu_p = 0.5$  eV and various value of the chemical potential.

F. S. Guimarães, A. T. Costa, R. B. Muniz, and M. S. Ferreira, *ibid.*, **84**, 195411 (2012); H. Lee, E. R. Mucciolo, G. Bouzerar, and S. Kettemann, arXiv:1204.5006.

- 15 S. Saremi, Phys. Rev. B **76**, 184430 (2007).
- 16 M. Sherafati and S. Satpathy, Phys. Rev. B **83**, 165425 (2011); *ibid* **84**, 125416 (2011).
- 17 G. Bergmann, Phys. Rev. B **36**, 2469 (1987); A. Jagannathan, E. Abrahams, and M. J. Stephen, *ibid.*, **37**, 436 (1988).
- 18 G. Zaránd and B. Janko, Phys. Rev. Lett **89**, 047201 (2002).
- 19 Q. Liu, C.-X. Liu, C. Xu, X.-L. Qi, and S.-C. Zhang, Phys. Rev. Lett **102**, 156603 (2009).
- 20 D. A. Abanin and D. A. Pesin, Phys. Rev. Lett **106**, 136802 (2011).
- 21 M. Zareyan, H. Mohammadpour, and A. G. Moghaddam, Phys. Rev. B **78**, 193406 (2008); Y. Asano, T. Yoshida,

- Y. Tanaka, and A. A. Golubov, Phys. Rev. B **78**, 014514 (2008); J. Linder, T. Yokoyama, D. Huertas-Hernando, and A. Sudbø, Phys. Rev. Lett. **100**, 187004 (2008); A. G. Moghaddam and M. Zareyan *ibid* **105**, 146803 (2010); D. A. Abanin *et al.*, Science **332**, 328 (2011).
- 22 V. K. Dugaev, V. I. Litvinov, and J. Barnas, Phys. Rev. B **74**, 224438 (2006); B. Uchoa *et al.*, Phys. Rev. Lett. **101**, 026805 (2008).
- 23 N. Tombros *et al.*, Nature (London) **448**, 571 (2007).
- 24 N. M. R. Peres, F. Guinea, and A. H. Castro Neto, Phys. Rev. B **72**, 174406 (2005).
- 25 Y.-W. Son, M. L. Cohen, and S. G. Louie, Nature (London) **444**, 347 (2006).
- 26 G. W. Semenoff, Phys. Rev. Lett. **53**, 2449 (1984).
- 27 L. M. Malard, J. Nilsson, D. C. Elias, J. C. Brant, F. Plentz, E. S. Alves, A. H. Castro Neto, and M. A. Pimenta, Phys. Rev. B **76**, 201401 (2007).
- 28 S. Chesi and D. Loss, Phys. Rev. B **82**, 165303 (2010).

<sup>29</sup> H. Imamura , P. Bruno, and Y. Utsumi, Phys. Rev. B 69, 121303(R) (2004)

<sup>30</sup> J. Fields, Math. Comp. 26, 757 (1972).